3-D ANALYSIS TO EVALUATE THE EFFECT OF SOIL IMPROVEMENT ON LIQUEFACTION OF MAN-MADE ISLAND

Atsushi YASHIMA[1], Fusao OKA[2] And Hiroki KANAMI[3]

SUMMARY

It has been observed that the man-made island called Port Island was extensively liquefied during the 1995 Hyogoken-Nambu Earthquake in Kobe. The interesting point is that the area improved by sand drain in Port Island was not heavily liquefied. In order to understand the increase in the soil strength and stiffness due to sand drain improvement, the seismic tomography investigation was carried out after the Kobe earthquake over the improved and unimproved area in Port Island. It is found that higher shear wave velocity was measured in the improved area than in the unimproved area. A three-dimensional effective-stress based finite element analysis was carried out in order to evaluate the effect of soil improvement by sand drain on liquefaction. Numerical analysis shows that liquefaction of improved area by sand drain is not significant compared with the unimproved area constructed by dropping soil on the sea bed from the barge.

INTRODUCTION

Port Island is an artificial island due south of Kobe central business district. It has been observed that Port Island was heavily liquefied during the 1995 Hyogoken-Nambu Earthquake in Kobe. This earthquake revealed that a weathered granite soil "Masado" can liquefy, although Masado has been considered to be generally resistant to liquefaction. Masado was used for reclamation in the first phase of Port Island. Masado has a relatively high fines content. The soil mineralogy of the fines content of Masado through 0.075 mm sieve was detected by using the X-ray diffractometer. Figure 1 shows the intensity of radiation normalized by the maximum intensity. From Figure 1, it is found that a small amount of clay minerals are included in fines content of Masado. The fines content of Masado consists of ground quartz and feldspar. This is one of the reasons for low liquefaction strength of Masado.

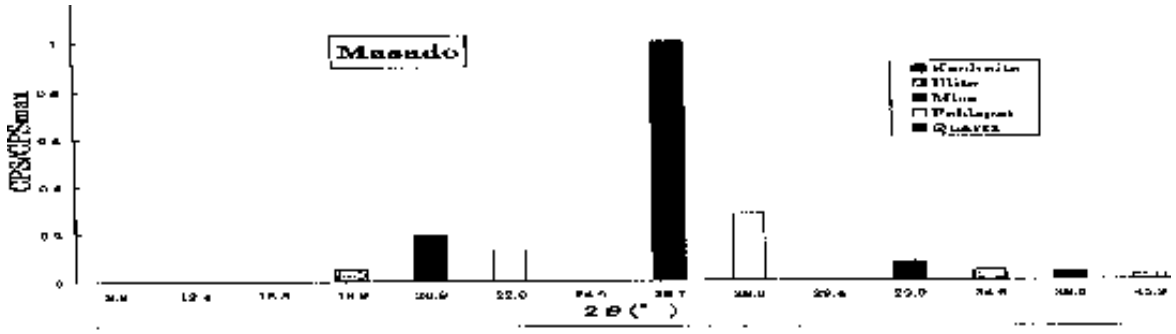

Figure 1: X-ray diffractometer chart for fines content of Masado.

The island were improved by several methods, such as sand drain, and compaction pile, or rod compaction method indicated in Figure 2 (Shibata et al. 1996). The interesting point is that the area improved by sand drain was not heavily liquefied illustrated in Figure 2. In fact, the settlement is not so large as that of unimproved area

[1] *Department of Civil Engineering, Gifu University, Japan, Email : yashima@cc.gifu-u.ac.jp*
[2] *Department of Civil Engineering, Kyoto University, Japan, Email : foka@nakisuna.kuciv.kyoto-u.ac.jp*
[3] *Tsuchiya-gumi Co. Ltd., Japan*

shown in Figure 3 (Yasuda et al. 1996), and the building was not heavily damaged. It has been pointed out that the improvement by driving sand drain is effective for preventing the liquefaction of ground. The sand drain was originally used for the acceleration of settlement of clay layers beneath the land fill material composed of Masado.

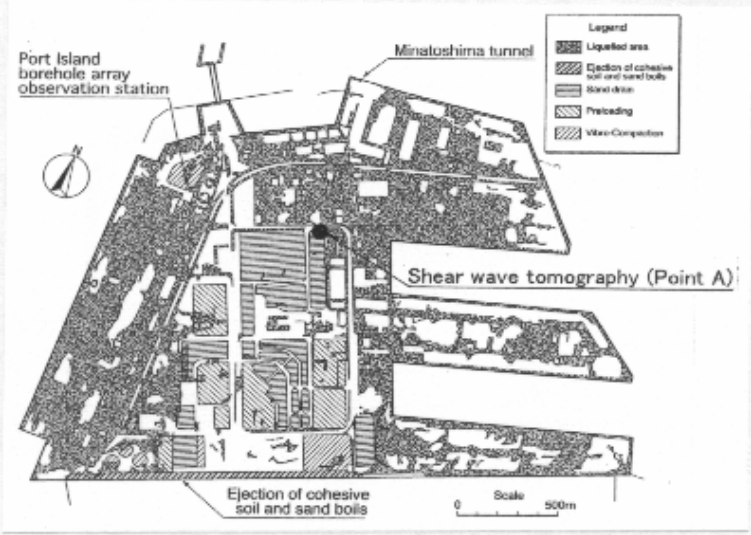

Figure 2: Distribution of liquefaction on Port Island (Shibata et al. 1996).

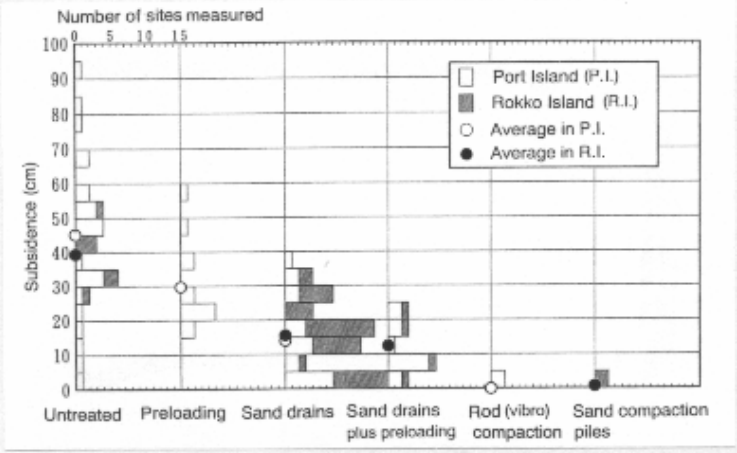

Figure 3: Comparison of ground subsidence in zones treated with different methods (Yasuda et al. 1996).

The aim of the present study is to clarify the effect of soil improvement by sand drain on liquefaction potential of reclaimed ground. A three-dimensional analysis of Port Island including sea bed which were modelled by the cyclic elasto-plastic constitutive equation with non-linear kinematical hardening rule was carried out. In the FEM analysis, the brick elements were used and the transportation of water through soil was considered using the numerical code LIQCA which is the effective stress based liquefaction analysis tool developed by the authors (Oka et al. 1994).

We have considered the increase in the soil stiffness and strength by the sand drain method as the increase in the shear wave velocity in the effective stress based liquefaction analysis. It is not so easy to evaluate the increase of strength by the standard penetration test at several points because of the large scattering. The increase in the soil strength and stiffness was evaluated through the average value of shear wave velocity observed in the seismic tomography performed after the Kobe Earthquake over the improved and unimproved area in Port Island. In the numerical analysis, it was found that the liquefaction potential of improved area by sand drain is not significant compared with the unimproved ground constructed by dropping soil on the sea bed from the barge.

SEISMIC TOMOGRAPHY AND ANAYTICAL METHOD

The distribution of shear wave velocity over the improved and unimproved area from the ground surface down to G.L.-35 m was obtained by using seismic tomography technique (Tsukamoto et al. 1997, Tanimoto et al. 1998). The detail of the layout of the boreholes around Point A indicated in Figure 2 is shown in Figure 4. Point A is situated on the border between the improved and unimproved area. The No.2 borehole is the source borehole and No.2 and 3 boreholes are receiver boreholes. The distribution of the shear wave velocity over the improved and unimproved area is shown in Figure 5. It is found that higher shear wave velocity was measured in the improved area than in the unimproved area.

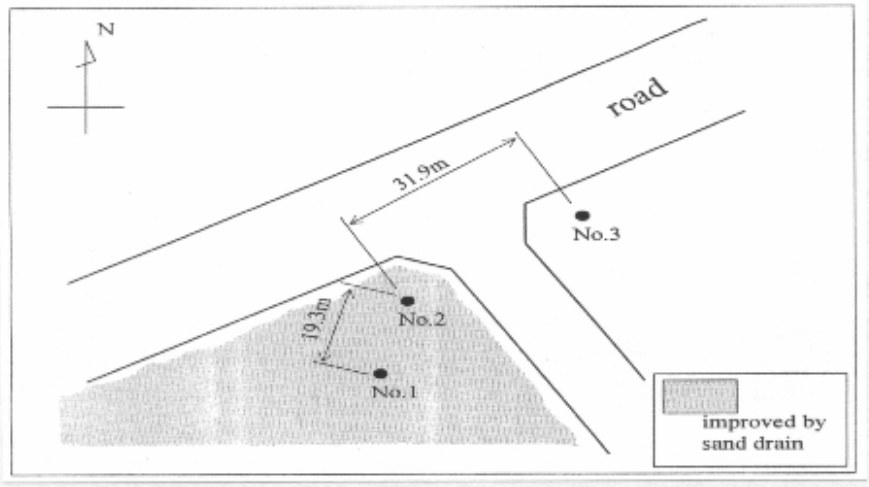

Figure 4: Detail of the layout of the boreholes around Point A indicated in Figure 2.

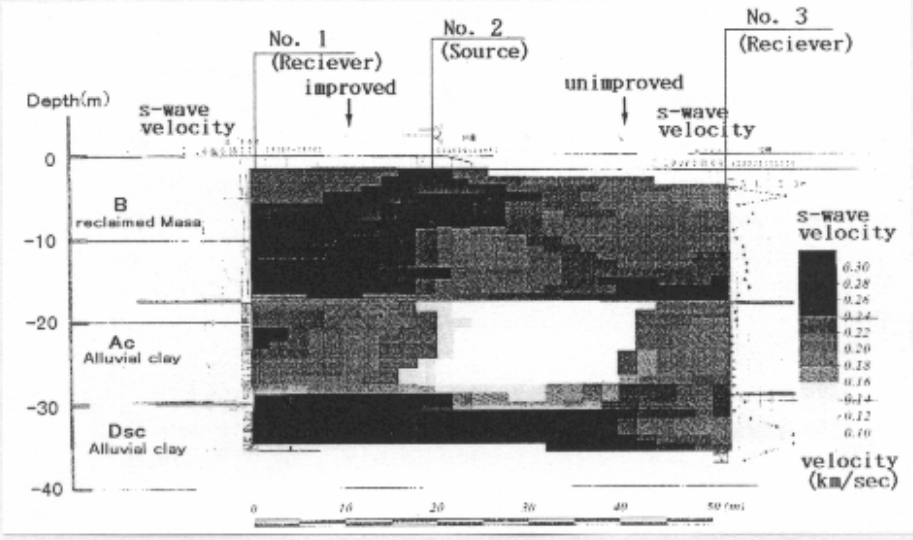

Figure 5: Distribution of shear wave velocity (Tsukamoto et al. 1997, Tanimoto et al. 1998).

The soil strength and stiffness are known to depend on the shear wave velocity of soil. The liquefaction strength and shear stiffness of the reclaimed soil and alluvial clay were determined based on the shear wave velocity. The material parameters in the cyclic elasto-plastic constitutive model (Oka et al.,1992; Tateishi et al. 1995) were optimized by using predicted liquefaction strength and shear stiffness. The material parameters used in the numerical analysis are summarized in Table 1 for the unimproved ground and Table 2 for the improved ground, respectively.

The reclaimed island was modeled as a rectangular parallelepiped (2km wide, 2km long and 19m deep), whose volume was nearly equivalent to that of the first stage reclamation in Port Island. The ground from G.L.-19 m to G.L.-83 m was modeled as natural deposit layers, 6km wide and 6km long. Ground model used in the analysis is shown in Figure 6. All ground layers were assumed as level layers. The boundary displacement conditions are

Table 1: Material parameters for the unimproved ground.

Depth (GLm)▲	Soil type	Void ratio e	Unit Weight (tf/m³□ □SPT□	Shear wave velocity V_S (m/sec)	Poiss-on's ratio υ	Coefficient Of permea-bility (m/sec)	G_0/σ'_{m0}	Phase trans-formation angle degree□°□(stress ratio M_m^*)	Failure angle degree(°□(stress ratio M_f^*□	Lique-faction strength Nc=10	Lique-faction strength Nc=30	Plastic modulus parameters upper:B_0^* lower:C_f^*	Plastic modulus parameters B_1^*	Dilatancy parameters Upper:D_0^* lower: n	Reference strain upper:$\gamma^{E*}_{DA\gamma}$ lower:$\gamma^{P*}_{DA\gamma}$
1 0.0 □	sandy gravel (reclaimed)	0.6	2.0 (5.2)	140	0.25		3350	25.2 (0.810)				50000 50000	1000	0.0	∞ ∞
2 -2.4	Sandy gravel (reclaimed)	0.6	2.0 (5.2)	180	0.25	3.0×10^{-5}	1700	22.4 (0.71)	25.2 (0.81)	0.22	0.17	8000 2000	800	0.6 2.8	0.0050% 0.0500%
3 -5.0	sandy gravel (reclaimed)	0.6	2.0 (6.5)	195	0.25	3.0×10^{-5}	1050	23.5 (0.75)	26.4 (0.85)	0.22	0.17	6000 2000	600	0.8 2.8	0.0050% 0.1000%
4 -8.8	sandy gravel (reclaimed)	0.6	2.0 (6.5)	195	0.25	3.0×10^{-5}	1050	23.5 (0.75)	26.4 (0.85)	0.22	0.17	6000 2000	600	0.8 2.8	0.0050% 0.1000%
5 -12.6	Sand with gravel (reclaimed)	0.6	2.0 (6.5)	220	0.25	3.0×10^{-5}	820	23.5 (0.75)	26.4 (0.85)	0.22	0.17	5000 2000	500	0.8 2.7	0.0050% 0.1000%
6 -15.8 ▲	Sand with gravel (reclaimed)	0.6	2.0 (6.5)	220	0.25	3.0×10^{-5}	820	23.5 (0.75)	26.4 (0.85)	0.22	0.17	5000 2000	500	0.8 2.7	0.0050% 0.1000%
7 -19.0	Alluvial clay	1.5	1.7 (3.5)	180	0.3	2.0×10^{-6}	350	(0.75)	(1.51)			8000 10000	160	0.0	∞ ∞
8 -23.0	Alluvial clay	1.5	1.7 (3.5)	180	0.3	2.0×10^{-6}	350	(2.5)	(1.51)			8000 10000	160	0.0	∞ ∞
9 -27.0	Alluvial sand	0.6	2.0 (13.5)	245	0.25	2.0×10^{-5}	615	28.0 (0.91)	31.4 (1.03)	0.4	0.30	6500 2000	650	0.8 3.0	0.0200% 0.1000%
10 -30.0 ▲	Alluvial sand	0.6	2.0 (13.5)	245	0.25	2.0×10^{-5}	615	28.0 (0.91)	31.4 (1.03)	0.4	0.30	6500 2000	650	0.8 3.0	0.0200% 0.1000%
11 -33.0	Pleistocene sandy gravel	0.5	2.0 (36.5)	305	0.25	1.0×10^{-5}	700	35.0 (1.16)	42.0 (1.41)	0.45	0.35	7000 2000	700	0.8 2.5	0.0200% 0.1000%
12 -41.5	Pleistocene sandy gravel	0.5	2.0 (36.5)	305	0.25	1.0×10^{-5}	700	35.0 (1.16)	42.0 (1.41)	0.45	0.35	7000 2000	700	0.8 2.5	0.0200% 0.1000%
13 -50.0	Pleistocene sandy gravel	0.5	2.0 (61.9)	350	0.25	1.0×10^{-5}	580	35.0 (1.16)	46.6 (1.57)	0.6	0.40	7000 2000	700	0.5 3.0	0.0200% 0.0100%
14 -61.0	Pleistocene Clay	1.2	1.75 (11.7)	303	0.3	1.0×10^{-6}	365	(2.43)	(1.43)			8000 10000	160	0.0	∞ ∞
15 -70.0	Pleistocene Clay	1.2	1.75 (11.7)	303	0.3	1.0×10^{-6}	365	(2.43)	(1.43)			8000 10000	160	0.0	∞ ∞
16 -79.0 ▲	Pleistocene sandy gravel	0.5	2.0 (68.0)	320	0.25	1.0×10^{-5}	410	35.0 (1.16)	46.6 (1.57)	0.6	0.40	7000 2000	700	0.6 2.3	0.0500% 0.1000%
-83.0	Note 1. ▲ accelerometer □2. K_0=0.5														

Table 2: Material parameters for the improved ground.

Depth (GL m)▲	Soil type	Unit Weight (tf/m³□ (SPT)	Shear wave velocity V_S (m/sec)	Poiss-on's ratio υ	Coefficient of permea-bility (m/sec)	G_0/σ'_{m0}	Phase trans-formation Stress ratio M_m^*	Failure stress ratio M_f^*	Lique-faction strength Nc=10	Lique-faction strength Nc=30	Plastic Modulus Parameters Upper:B_0^* lower:C_f^*	Plastic Modulus Parameters B_1^*	Dilatancy parameters upper: D_0^* lower: n	Reference strain upper:$\gamma^{E*}_{DA\gamma}$ lower:$\gamma^{P*}_{DA\gamma}$
1 0.0 □	sandy gravel (reclaimed)	2.0 (5.2)	140	0.25		3350	0.81				66500 50000	1300	0.0	∞ ∞
2 -2.4	sandy gravel (reclaimed)	2.0 (12.3)	240	0.25	3.0×10^{-5}	2890	0.88	1	0.4	0.3	9500 2000	950	0.1 10.0	0.020% 0.1000%
3 -5.0	sandy gravel (reclaimed)	2.0 (15.4)	260	0.25	3.0×10^{-5}	2230	0.94	1.06	0.4	0.3	7000 2000	700	0.1 12.0	0.020% 0.1000%
4 -8.8	sandy gravel (reclaimed)	2.0 (19.2)	280	0.25	3.0×10^{-5}	1832	1.02	1.12	0.4	0.3	7000 2000	700	0.7 10.0	0.020% 0.1000%
5 -12.6	sand with gravel (reclaimed)	2.0 (16.5)	300	0.25	3.0×10^{-5}	1655	0.97	1.66	0.4	0.3	6000 2000	600	0.7 14.0	0.020% 0.1000%
6 -15.8 ▲	sand with gravel (reclaimed)	2.0 (16.5)	300	0.25	3.0×10^{-5}	1391	0.97	1.66	0.4	0.3	6000 2000	600	0.7 14.0	0.020% 0.1000%
7 -19.0	Alluvial clay	1.7 (4.8)	200	0.3	2.0×10^{-6}	456	0.85	0.79			9000 10000	160	0.0	∞ ∞
8 -23.0	Alluvial clay	1.7 (4.8)	200	0.3	2.0×10^{-6}	405	0.85	0.79			9000 10000	160	0.0	∞ ∞

free except the bottom surface. The ground water level (G.L.-2.4 m) in the reclaimed island and the seabed surface (G.L.-19 m) were drained boundaries, while the bottom and lateral surface were undrained boundaries. About 600 brick elements were used for the modeling, which were rather flat and simplified shape. The inclination of soil layer and the variation of input seismic motion at a depth were not considered. It could be, however, possible to obtain an approximate behavior of the reclaimed island and its surroundings. Although the distribution of the improved area in Port Island is rather complex (Figure 2), the simplified rearrangement of the improved area was treated as shown in Figure 7. Although several improving techniques were used in Port Island, same material parameters shown in Table 2 were used for the whole improved area in the present analysis.

The borehole array record in Port Island obtained during the 1995 Hyogoken-Nambu earthquake was used for the analytical input motion. The borehole array observation station is located at the northeast of Port Island indicated in Figure 2. Three dimensional acceleration records at G.L. –83m and were used.

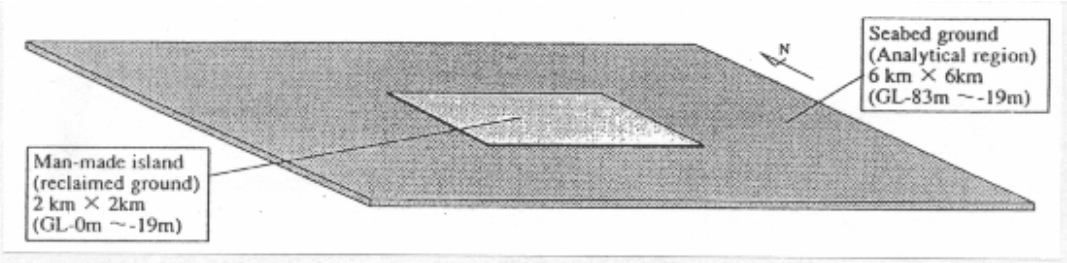

Figure 6: Ground model used in the analysis.

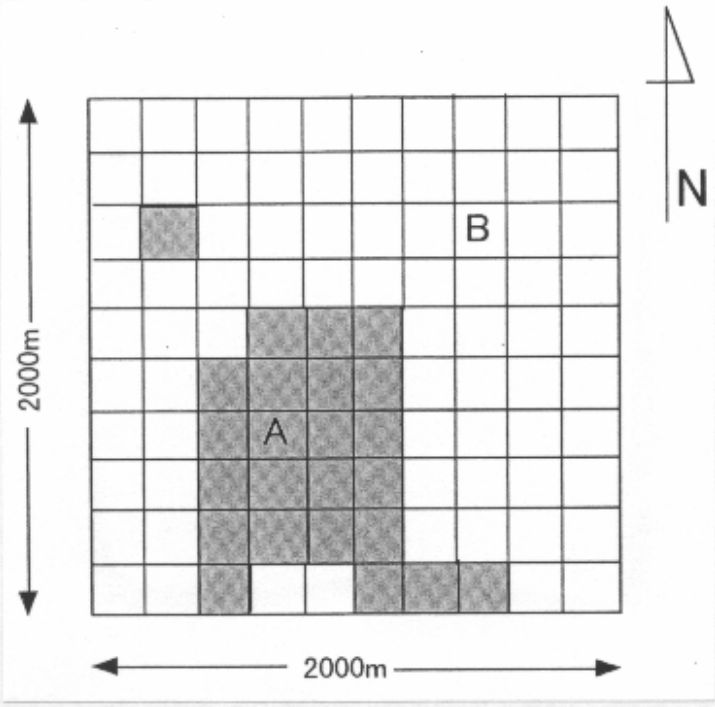

Figure 7: Simplified rearrangement of the improved area in the analysis.

ANALYTICAL RESULTS AND DISCUSSIONS

The distribution of the relative change of effective stress ($(\sigma'_{m0} - \sigma'_m)/\sigma'_{m0}$; σ'_{m0} is the initial mean effective stress and σ'_m is the current mean effective stress) at the end of shaking (t=15 sec.) is shown in Figure 8. Note that at the initial state, that is, $\sigma'_m = \sigma'_{m0}$, the relative change of effective stress is 0.0. On the other hand, once the ground is liquefied, that is, $\sigma'_m = 0$, the relative change of effective stress is 1.0. It is seen from Figure 8 that higher value of relative change of effective stress (over 0.7) is distributed in the reclaimed ground below the water level and the alluvial sand layer. The distribution of relative change of effective stress at the ground level at G.L.-5.0 m is also shown in Figure 9. The distribution is not uniform due to the existence of the improved area. It is found that the relative change of effective stress in the improved area at this ground level is much smaller than that in the unimproved area.

Time histories of relative change of effective stress for selected points at G.L.-5m (close to the ground water table) as well as G.L.-16m (almost bottom of reclaimed ground) are also shown in Figure 10. The selected points are in the improved area indicated as Point A in Figure 7 and in the unimproved area indicated as Point B in Figure 7. From Figure 10, significant differences in the build-up process of the excess pore water pressure could not be obtained at G.L.-16m. On the other hand, at G.L.-5m, the built-up process of the excess pore water pressure is very different. Remarkable development of excess pore water pressure was suppressed in the improved area due to the high liquefaction strength and shear stiffness. It is found that the liquefaction potential of improved area of the upper part of reclaimed ground by sand drain is not significant compared with the unimproved ground.

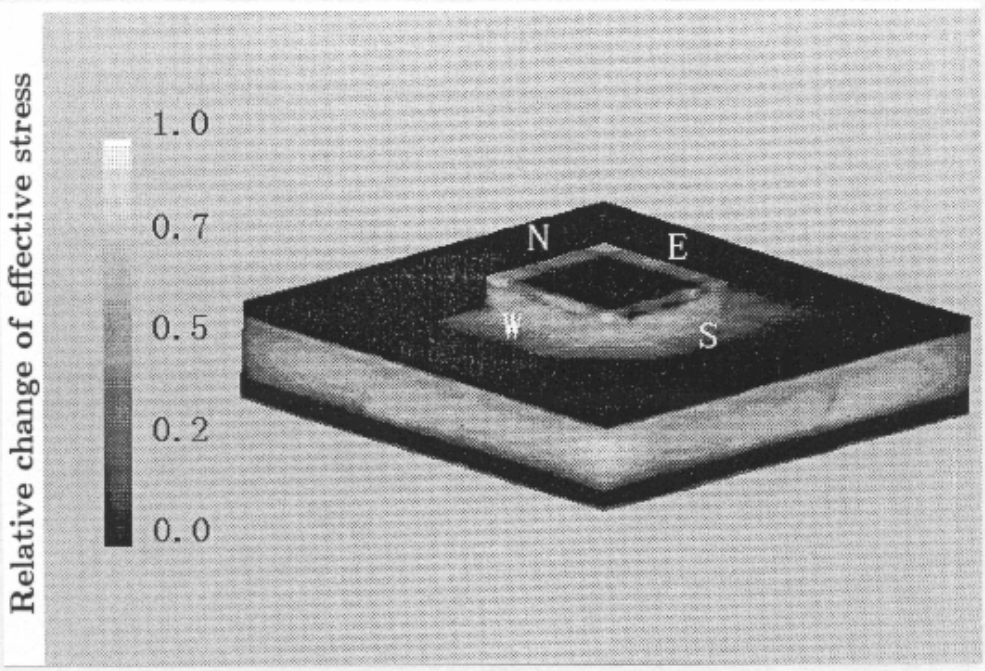

Figure 8: Distribution of relative change of effective stress in the whole analytical area at the end of shaking (t=15 sec.).

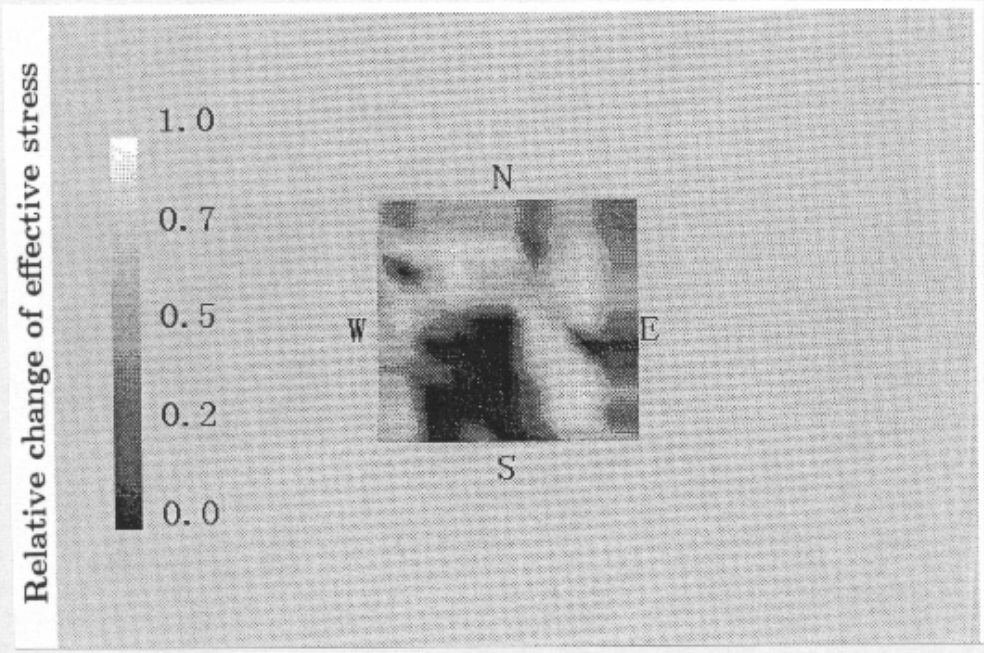

Figure 9: Distribution of relative change of effective stress at the ground level at G.L. –5.0 m at the end of shaking (t=15 sec.).

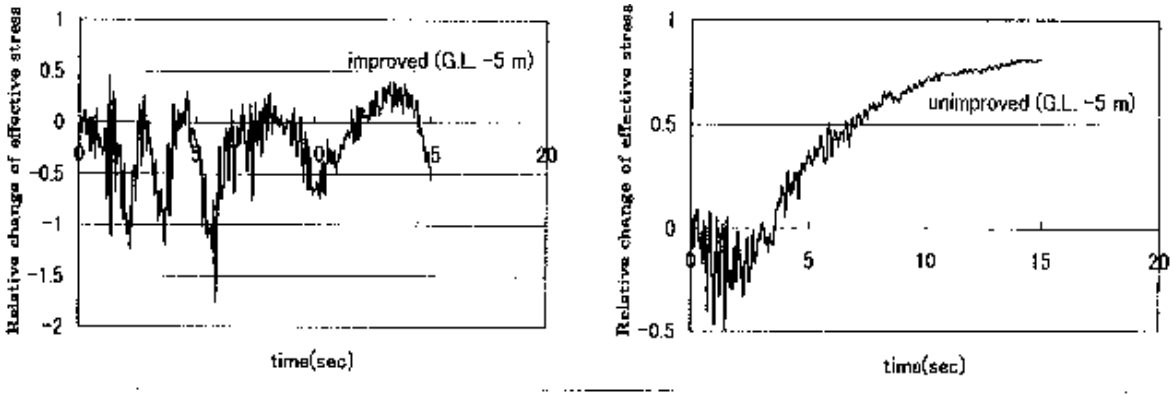

Figure 10(a): Time histories of relative stress change of effective stress for Points A and B shown in Figure 5 at G.L. –5 m.

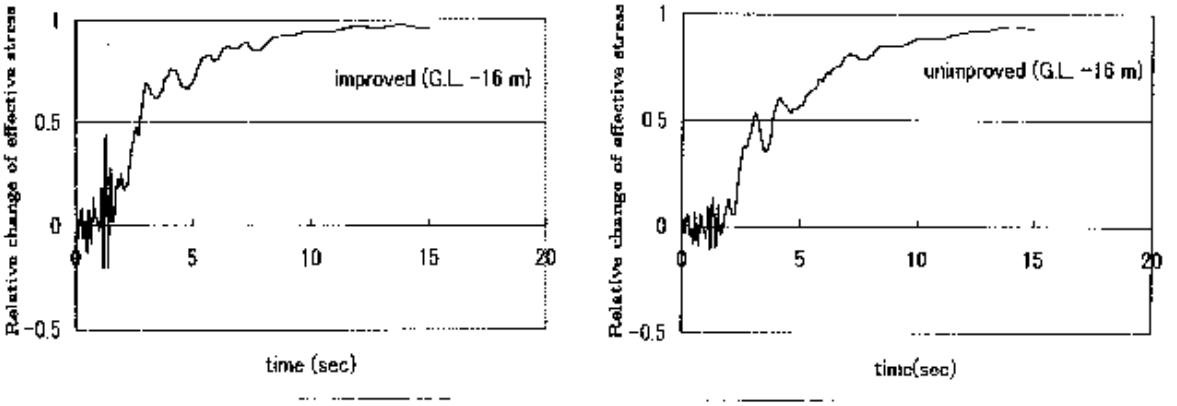

Figure 10(b): Time histories of relative stress change of effective stress for Points A and B shown in Figure 5 at G.L. –16 m.

CONCLUSIONS

1. In order to understand the increase in the soil strength and stiffness due to sand drain improvement, the seismic tomography investigation was carried out after the Kobe earthquake over the improved and unimproved area in Port Island. The distribution of shear wave velocity from the ground surface down to G.L.-35 m was obtained. It is found that a higher shear wave velocity was measured in the improved area than in the unimproved area.
2. An effective-stress based three-dimensional finite element analyses were carried out to valuate the effect of soil improvement by sand drain on liquefaction potential of reclaimed island based on the shear wave velocity measurement.
3. Sand and clayey layers in Port Island including sea bed were modeled by the cyclic elasto-plastic constitutive equation with non-linear kinematical hardening rule. In the FEM analysis, the brick elements were used and the transportation of water through soil was considered.
4. From the numerical analysis, it was found that the liquefaction potential of improved area by sand drain is not significant compared with the unimproved ground constructed by dropping soil on the sea bed from the barge.

REFERENCES

Oka,F., Yashima,A., Kato,M. and Sekiguchi,K. (1992), "A constitutive model for sand based on the non-linear kinematic hardening rule and its application," *Proc. 10th WCEE*, pp2529-2534.

Oka,F., Yashima,A., Shibata,T., Kato,M. and Uzuoka,R. (1994), "FEM-FDM coupled liquefaction analysis of a porous soil using an elasto-plastic model," *Applied Scientific Research*, 52, pp209-245.

Shibata,T., Oka,F. and Ozawa,Y. (1996), “Characteristics of ground deformation due to liquefaction,” *Special Issue of Soils and Foundations*, pp65-79.
Tanimoto,K., Takahashi,Y., Murata,Y., Yamamoto,M. and Sugawara,N. (1998), “Examination of liquefaction potential by seismic tomography after the Hyogoken-Nambu Earthquake in the reclaimed land of Kobe,” *Proc. Int. Conf. On Site Characterization*, ISSMGE, Atlanta, pp531-536.
Tateishi,A., Taguchi,Y., Oka,F. and Yashima,A. (1995), “A cyclic elasto-plastic model for sand and its application under various stress conditions,” *Proc. 1st Int. Conf. on Earthquake Geotechnical Eng., IS-Tokyo'95*, pp399-404.
Tsukamoto,T., Nakajima,S., Yamamoto,M. and Murata,Y. (1997), “Evaluation on liquefaction potential by seismic tomography after the earthquake event in the reclaimed land of Kobe,” *OYO Technical Report, Special Issue on Hyogoken-Nambu Earthquake*, pp215-235.
Yasuda,S., Ishihara,K., Harada,K. and Shinkawa,N. (1996), “Effect of soil improvement on ground subsidence due to liquefaction